Crossover from photon to exciton-polariton lasing

Elena Kammann, Hamid Ohadi, Maria Maragkou, Alexey V Kavokin and Pavlos G Lagoudakis[1]

School of Physics and Astronomy, University of Southampton,
Southampton SO17 1BJ, UK
E-mail: Pavlos.Lagoudakis@soton.ac.uk

Abstract. We report on a real-time observation of the crossover between photon and exciton-polariton lasing in a semiconductor microcavity. Both lasing phases are observed at different times after a high-power excitation pulse. Energy-, time- and angle-resolved measurements allow for the transient characterization of carrier distribution and effective temperature. We find signatures of Bose–Einstein condensation, namely macroscoping occupation of the ground state and narrowing of the linewidth in both lasing regimes. The Bernard–Douraffourgh condition for inversion was tested and the polariton laser as well as the photon laser under continuous wave excitation were found to operate at estimated densities below the theoretically predicted inversion threshold.

[S] Online supplementary data available from stacks.iop.org/NJP/14/105003/mmedia

Bose–Einstein condensation (BEC) of exciton-polaritons in semiconductor microcavities [1–3] and photons in dye-filled microcavities operating in the weak exciton–photon coupling regime [4] have been reported in recent years. Unlike atomic condensates in harmonic traps [5, 6], where a coherent state is achieved by cooling down of the bosonic thermal distribution, the condensates (coherent states) of polaritons can be formed without thermal equilibrium for example by parametric amplification [7] or under nonresonant excitation at negative detunings [2]. Moreover, the spectra of vertical cavity surface emitting semiconductor lasers (VCSELs) frequently show thermal tails coexisting with the lasing mode [8] that suggest

---

[1] Author to whom any correspondence should be addressed.

thermal equilibrium of photons [9]. Essentially the experimental observations of polariton BEC in the strong-coupling regime [1], photon BEC in the weak-coupling regime [4] and weak-coupling lasing or VCSEL operation [8, 10] have very similar signatures. Carriers are distributed according to the Bose–Einstein distribution, the emission narrows in energy and the first-order spatial coherence builds up. Recently we showed that spontaneous symmetry breaking, which is the Landau criterion for the phase transition, can also be observed in polariton and photon lasers [11].

However, the physical processes by which condensation and conventional lasing occur are fundamentally different. Condensation is a purely thermodynamic phase transition during which the total free energy of the system is minimized, whereas conventional lasing is a balance between the gain from inversion and the loss in the system. In a conventional semiconductor laser, lasing occurs by the stimulated emission of the cavity photons from the electron–hole plasma. Above a threshold density, the stimulated emission becomes faster than the thermalization rate. As a result, a dip is formed in the carrier distribution, which is called kinetic hole burning [12]. This is because the thermalization process can no longer supply the lost carriers at sufficient speed. In condensation, however, the system remains thermalized while lasing. The question of whether the term BEC or lasing is appropriate for degenerate condensates of exciton polaritons and photons is still a subject of debate in the scientific community [13–15].

The crossover from strong to weak coupling according to the coupled oscillator model takes place when the exciton–photon coupling strength (g_0) equals half of the difference between the decay rates of cavity photons (γ_{cav}) and excitons (γ_{exc}) [16]. This may be achieved by changing the optical pumping strength. The exciton linewidth increases and the oscillator strength decreases with the increase of pumping intensity, which brings the system from strong to weak coupling. This transition is not to be confused with the Mott transition from an exciton gas to an electron–hole plasma [17–20]. Whilst the distinction between strong and weak coupling in a microcavity is straightforward, as the dispersion relations exhibit specific differences, it is very hard to identify the exact point of the Mott transition by photoluminescence spectroscopy. A transition to the weak-coupling regime with increasing pumping strength in steady state has been observed by several groups and the carrier densities at the onset of photon lasing compare well with the Mott density [21–25]. This paper adds to this body of work as it investigates the dynamical transition from the weak to the strong exciton-light coupling regime in a planar semiconductor microcavity excited by a short high-power excitation pulse. We particularly investigate the distributions of carriers during this crossover and discuss the possibility of a BEC of photons. We observe clear features of polariton and photon lasing and find quasi-thermal distributions of quasiparticles in the weak- and in the strong-coupling regime, which could imply BEC of photons and polaritons. A closer look at the temporal dynamics and the change of the effective temperatures during the transition provide insight into the nature of the observed lasing modes and the thermodynamic state of the system. We further investigate the build-up of photon lasing under continuous wave (CW) excitation and investigate the question of whether the system is inverted by means of the Bernard–Douraffourg condition for lasing.

The system under study is a GaAs microcavity grown by molecular beam epitaxy. Previous works have shown that lasing in the weak coupling can be observed in this sample under CW excitation [10], whilst nonlinearities in the strong-coupling regime are accessible under pulsed excitation, as sample overheating is strongly reduced [26]. At higher excitation power the emission switches to the weak-coupling regime, similar to the observations in [25]. We show
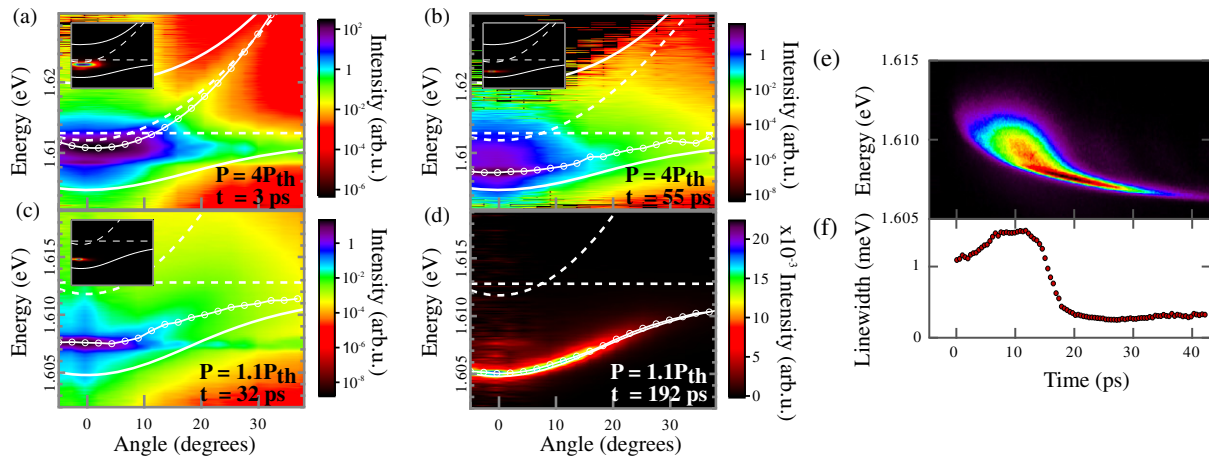
Figure 1. Dispersion images at different times and excitation powers. (a)–(d) Dispersions at excitation powers of $P = 4P_{th}$ (a, b) and $P = 1.1P_{th}$ (c, d) at 3 ps (a), 55 ps (b), 32 ps (c) and 192 ps (d). The insets in (a)–(c) show the same dispersions but in linear color scale. At $P = 4P_{th}$ a transition from the weak- to the strong-coupling regime is clearly observed between (a) and (b), whilst at lower excitation powers a blue shifted exciton-polariton laser at early times relaxes towards the modes of the linear strong-coupling regime. Images are bilinearly interpolated. The solid lines indicate the shape of the modes at low excitation powers and the dashed lines are the corresponding bare exciton and cavity modes. The white circles follow the location of maxima corresponding to the measured photon and exciton-polariton modes. (e) Typical energy-resolved evolution of the ground state emission intensity for $P = 8P_{th}$. (f) Linewidth as a function of time.

that the photon and polariton lasing occur at different times after the excitation pulse and that at high powers photon lasing is followed by polariton lasing. Experiments were carried out using a liquid helium cooled wide-field view cold finger cryostat. The exciton–cavity mode detuning was set to -0.5 meV. Transform limited pulses from a femtosecond Ti:Sapphire oscillator tuned to a reflection minimum of the Bragg mirror were focused to a 30 μm spot through an objective with a high numerical aperture (NA = 0.7). The dispersion relation was imaged through the same objective onto the slit of a monochromator equipped with a water cooled charge coupled device (CCD) and a streak camera with ps resolution. For temporal resolution the momentum space was scanned across the crossed slits of the streak camera and the monochromator.

Figure 1(a) shows a snapshot of a bi-linearly interpolated image of the microcavity dispersion 3 ps after optical excitation at the excitation density $P = 4P_{th}$ (where $P_{th} = 7$ mW is the power threshold for lasing). The photoluminescence intensity is displayed in false-color logarithmic scale. The inset of figure 1(a) shows the same microcavity dispersion in false-color linear scale. Solid white lines indicate the exciton-polariton branches in the linear regime and the dashed lines show the bare cavity and exciton modes. Observation of the bare cavity photon dispersion confirms that the excitation pulse brings the microcavity to the weak-coupling regime. Figure 1(b) shows the same as figure 1(a) but at 55 ps after optical excitation. White circles indicate the intensity maxima of the recorded spectrum at each detection angle, following

the cavity (a) and the polariton mode (b). The lower exciton-polariton dispersion is uniformly blue-shifted due to the repulsive interaction with the exciton reservoir. It is instructive to compare these results with the lower excitation power sufficient to excite a polariton condensate. Figure 1(c) shows a snapshot of the microcavity dispersion 32 ps after optical excitation at the excitation density $P = 1.1 P_{th}$. Similarly to figure 1(b), a near uniformly blue-shifted lower exciton-polariton dispersion is observed. Figure 1(d) shows a snapshot of the microcavity dispersion at 192 ps under the same optical excitation, when the exciton-polariton dispersion in the linear regime is fully recovered as a result of the depletion of the exciton reservoir. Therefore, using time-resolved dispersion imaging we observe the dynamics of the transition of the microcavity eigenstates through three distinctively different regimes: from the weak-coupling regime where we observe a bare cavity mode, to the nonlinear strong-coupling regime featuring a blue-shifted lower exciton-polariton branch, through to the linear strong-coupling regime where the exciton-polariton dispersion is not altered spectrally (see supplementary movies, available at stacks.iop.org/NJP/14/105003/mmedia). The temporal evolution of the ground state energy is depicted in figure 1(e), showing the redshift of the emission with time. This reflects the transition from the weak- to the strong-coupling regime and can be understood as an effect of the depletion of the carrier reservoir. The emission linewidth reflects the coherence properties in the three regimes. Starting from a linewidth of ∼1 meV in the photon lasing regime the linewidth initially increases when the system enters the transitory regime and then narrows down to the linewidth of the polariton laser [27] (figure 1(f)). The time-resolved spectra and linewidth evolutions in the linear and nonlinear strong-coupling regime are given in the supplemental material 1 (available at stacks.iop.org/NJP/14/105003/mmedia). The time axis was rescaled to account for the temporal distortion caused by the use of the grating (for further information see the supplemental material 2).

Figure 2(a) shows the occupancy as a function of energy at different times for $P = 4 P_{th}$. At early times (3 ps), whilst still in the weak-coupling regime, we observe a massively occupied cavity mode ground state on top of a thermalized tail of excited states. In the transitory regime (10–54 ps) the dispersion cannot be mapped because the linewidth at higher angles is strongly broadened and therefore a distribution of population is unattainable. At later times, 55 and 76 ps after optical excitation whilst in the strong-coupling regime, we observe a largely occupied exciton-polariton ground state coexisting with a thermalized exciton-polariton gas. After ∼116 ps the ground state is no longer degenerate and the particle distribution is close to a Boltzmann distribution. At even later times, the occupation of the ground state cannot be resolved as it is four orders of magnitude lower than at the peak emission intensity. Figure 2(b) shows successive snapshots of the emission intensity of exciton polaritons as a function of energy for low excitation powers ($P = 1.1 P_{th}$). We observe a largely occupied ground exciton-polariton state on top of a thermalized exciton-polariton gas, in low-excitation nonlinear regime. The depletion of the ground state and the loss of thermalization occur around the same time (∼86 ps) as a bottleneck builds out (140 and 192 ps). Figure 2(c) shows the temporal evolution of temperature in the transition from photon to exciton-polariton condensate (green circles), and from polariton condensate to a thermalized exciton-polariton gas (red triangles). Effective temperatures were extracted by fitting a Bose–Einstein distribution to the measured angular distribution of the emission intensity [28] (dashed gray lines in figures 2(a) and (b)). This analysis provides insight into the thermodynamics of the system and how far away from thermal equilibrium the quasiparticles are. The effective temperature in the weak-coupling regime (∼32 K) is higher than in the strong-coupling regime (∼16 K), while in both cases
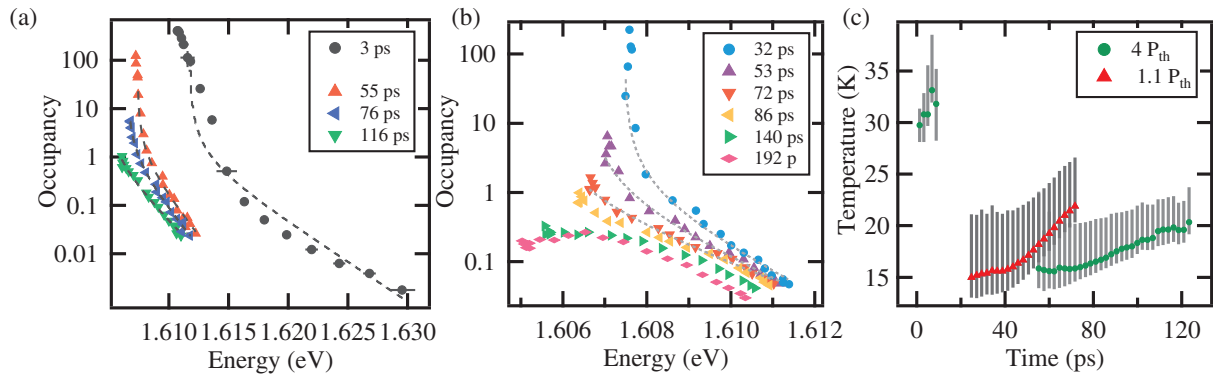
Figure 2. Energy distribution and temperatures. (a) The occupation measured at different energies is given for several times after the optical excitation for $P = 4P_{th}$. At 3 ps a photon laser at the energy of 1.610 eV coexists with thermalized photons at ~ 30 K populating the cavity dispersion. At 55 and 76 ps a Bose–Einstein distribution of exciton-polaritons with a degenerate ground state is observed. After 116 ps the occupancy of the ground state reaches one. (b) Analysis of the spectra for $P = 1.1 P_{th}$ at different angles and times show the coexistence of an exciton-polariton lasing mode at the ground state with a thermalized population at early times. We map the depletion of the condensate until the linear exciton-polariton regime, where the distribution exhibits a bottleneck. (c) The temporal evolution of temperature for $P = 1.1 P_{th}$ (red triangles) and $P = 4P_{th}$ (green circles). The dashed lines in (a) and (b) are Bose–Einstein fits with a spectral range of $> 3k_B T$.

the quasiparticles remain warmer than the lattice temperature (~ 6 K). The lower effective temperature of the polariton gas reflects the longer timescale on which they thermalize with respect to photons. At the formation stage of the photon laser, the effective photon temperature is higher (~ 32 K) than the subsequent exciton-polariton gas (~ 16 K).

The photon gas thermalizes via absorption and re-emission processes in the intracavity quantum wells, similar to the mechanism of photon thermalization in a dye-filled microcavity [9]. This thermalization mechanism is analogous to the exciton-polariton thermalization in the strong-coupling regime if the system is below the Mott transition and the excitons are still present in the weak-coupling regime. In this case each photon state has a finite exciton fraction even in the weak-coupling regime, which allows for efficient interaction with phonons and other dressed photons. On the other hand, the observed photon lasing mode occurs at much shorter times than the usual exciton formation rates of tens of picoseconds [29] in GaAs. In this case the thermalized distribution originates from the ultrafast self-thermalization of an electron–hole plasma (tens of femtoseconds) [30]. Thermalization and BEC in an ionized plasma is in principle possible [31], through Compton scattering.

Upon the formation of excitons the effective temperature approaches the lattice temperature through carrier phonon scattering in the picosecond timescale. Exciton polaritons have larger exciton fraction than the photons, which is why they interact more strongly with acoustic phonons and between themselves. The cooling of exciton polaritons occurs on a longer timescale providing a different temperature for the exciton-polariton gas with respect to that of
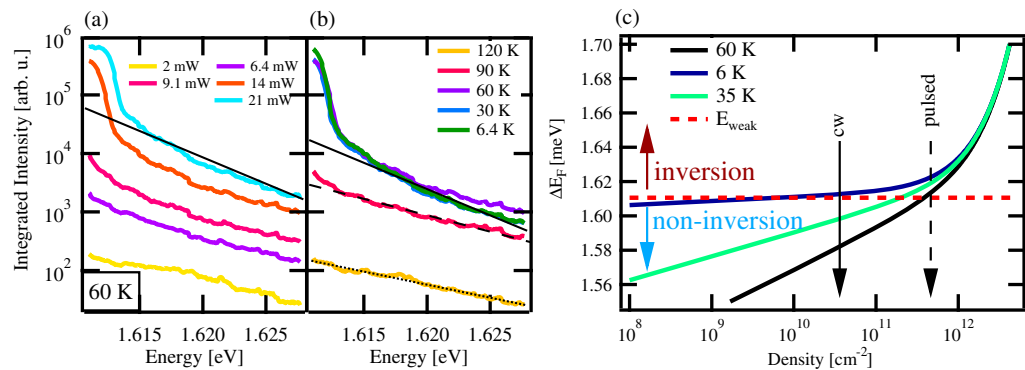
Figure 3. Photon lasing in the steady state. (a) At 60 K the distribution of photons thermalizes at a temperature close to the lattice temperature and the ground state becomes macroscopically occupied at a certain excitation power. (b) Photon distributions for different cryostat temperatures. The transition can equally be induced by lowering of the temperature. Photon distributions follow the lattice temperature and the ground state becomes degenerate around 60 K. While the lattice temperature can be varied down to ∼6 K the photon distribution does not go below 60 K. Straight lines indicate Boltzmann distributions for 60 K (solid), 95 K (dashed) and 120 K (dotted). (c) Difference between the Fermi levels of electrons and holes as a function of carrier density. For three different temperatures, corresponding to the cryostat temperature (6 K), the temperature in the weak coupling measured for pulsed excitation (35 K) and under CW excitation (60 K). The arrows indicate the experimental conditions.

the exciton reservoir and the host lattice. In the intermediate regime of the temporal transition from photon to exciton-polariton laser, the distinction between the weak- and strong-coupling regime in momentum space vanishes and the energy appears more and more red shifted, indicating broadband emission similar to the kind observed in [32] or the coexistence of polariton and photon lasing [33].

The buildup of the photon laser is below the temporal resolution of our detection apparatus. Therefore we show time-integrated photoluminescence spectra under CW excitation at different temperatures and excitation densities. Figure 3(a) shows pump power dependent data at 60 K. The distribution thermalizes at a temperature close to the lattice temperature (solid line) and upon saturation the ground state becomes macroscopically occupied, as observed in [4]. Next we induce the transition from a thermalized distribution to a photon laser by lowering the temperature, to demonstrate further similarities to atom [5, 6] and polariton condensates [2] (figure 3(b)). We use CW excitation at a constant excitation power and study the emission pattern of the cavity mode as a function of temperature. At a critical temperature of about 90 K the thermal distribution achieves the degeneracy threshold and photons start condensing at the cavity ground state. Although such behavior is characteristic of a thermodynamic phase transition, it is more likely due to the change of the cavity mode energy with respect to the electron hole transition energy in a similar fashion to VCSELs [34]. The temperature of the photon gas follows the lattice temperature between 60 and 120 K, but does not go below 60 K which is slightly above the exciton binding energy in bulk GaAs [20]. This might be an

indication that the electron–hole pairs are unbound in this case. In the time-resolved experiments we detect a lower temperature for the photon lasing (figure 2(c)), due to lesser heating of the sample under pulsed excitation.

Next we test the Bernard–Douraffourg condition for lasing [35] by comparing the emission energy in the weak-coupling regime (E_{weak}) with the difference between the Fermi energies (ΔE_{F}) of electrons in the conduction band and holes in the valence band for the weak-coupling regime. Conventional lasing occurs when $\Delta E_{\text{F}} > E_{\text{weak}}$. Calculations of the Fermi-energies and carrier densities are provided in the supplemental material 3 (stacks.iop.org/NJP/14/105003/mmedia). Figure 3(c) shows ΔE_{F} as a function of the density of electron hole pairs. Arrows indicate the experimental conditions. The system is close to the theoretically estimated inversion threshold, at the onset of photon lasing under pulsed excitation. However, the density in the CW case remains an order of magnitude below the inversion density predicted for 60 K, which is the lowest photon temperature measured under CW excitation. Further investigations are needed to obtain direct spectroscopic evidence of the carrier density under CW excitation.

In conclusion, we have studied the dynamic transition from a photon to a polariton laser following a high-power excitation pulse. Dispersion images clearly show the transition from the weak to the strong coupling. Both regimes exhibit the same signatures of BEC: a macroscopic occupation of the ground state on top of a thermalized tail, narrowing of the linewidth and narrowing of the distribution in momentum space. We have also shown that the transition to the photon laser can be induced by decreasing the temperature. The estimated carrier densities remain below the inversion threshold in the CW excitation regime as well as in the strong-coupling regime under pulsed excitation. The effective temperatures show how far from thermal equilibrium the system is at different times after the excitation pulse and the evolution of the linewidth maps the transition between two coherent states by a passage through an incoherent state. The results presented here as well as the recently reported observation of spontaneous symmetry breaking and long-range order [11] call for further studies of condensation in the weak-coupling regime. Direct spectroscopic evidence of free carrier and exciton densities is needed to unambiguously distinguish between photon lasing and BEC in the weak coupling regime.

References

[1] Kasprzak J *et al* 2006 Bose–Einstein condensation of exciton polaritons *Nature* **443** 409–14
[2] Kasprzak J, Solnyshkov D D, André R, Dang L S and Malpuech G 2008 Formation of an exciton polariton condensate: thermodynamic versus kinetic regimes *Phys. Rev. Lett.* **101** 146404
[3] Deng H, Weihs G, Santori C, Bloch J and Yamamoto Y 2002 Condensation of semiconductor microcavity exciton polaritons *Science* **298** 199–202

[4] Klaers J, Schmitt J, Vewinger F and Weitz M 2010 Bose–Einstein condensation of photons in an optical microcavity *Nature* **468** 545–8

[5] Davis K B, Mewes M-O, Andrews M R, van Druten N J, Durfee D S, Kurn D M and Ketterle W 1995 Bose–Einstein condensation in a gas of sodium atoms *Phys. Rev. Lett.* **75** 3969–73

[6] Anderson M H, Ensher J R, Matthews M R, Wieman C E and Cornell E A 1995 Observation of Bose–Einstein condensation in a dilute atomic vapor *Science* **269** 198–201

[7] Savvidis P G, Baumberg J J, Stevenson R M, Skolnick M S, Whittaker D M and Roberts J S 2000 Angle-resonant stimulated polariton amplifier *Phys. Rev. Lett.* **84** 1547–50

[8] van Exter M P, Jansen Van Doorn A K and Woerdman J P 1995 Effect of spatial filtering on the spontaneous emission spectrum of a sub-threshold VCSEL *IEEE J. Sel. Top. Quantum Electron.* **1** 601–5

[9] Klaers J, Vewinger F and Weitz M 2010 Thermalization of a two-dimensional photonic gas in a 'white wall' photon box *Nature Phys.* **6** 512–5

[10] Bajoni D, Senellart P, Lemaître A and Bloch J 2007 Photon lasing in GaAs microcavity: similarities with a polariton condensate *Phys. Rev.* B **76** 201305

[11] Ohadi H, Kammann E, Liew T C H, Lagoudakis K G, Kavokin A V and Lagoudakis P G 2012 Spontaneous symmetry breaking in a polariton and photon laser *Phys. Rev. Lett.* **109** 016404

[12] Yamaguchi M, Kamide K, Ogawa T and Yamamoto Y 2012 BEC–BCS-laser crossover in Coulomb-correlated electron–hole–photon systems *New J. Phys.* **14** 065001

[13] Butov L V and Kavokin A V 2012 The behaviour of exciton-polaritons *Nature Photon.* **6** 2

[14] Deveaud-Plédran B 2012 On the condensation of polaritons *J. Opt. Soc. Am.* B **29** A138–45

[15] Snoke D 2012 Polariton condensation and lasing arXiv:1205.5756

[16] Savona V, Andreani L C, Schwendimann P and Quattropani A 1995 Quantum well excitons in semiconductor microcavities: unified treatment of weak and strong coupling regimes *Solid State Commun.* **93** 733–9

[17] Kappei L, Szczytko J, Morier-Genoud F and Deveaud B 2005 Direct observation of the Mott transition in an optically excited semiconductor quantum well *Phys. Rev. Lett.* **94** 147403

[18] Stern M, Garmider V, Umansky V and Bar-Joseph I 2008 Mott transition of excitons in coupled quantum wells *Phys. Rev. Lett.* **100** 256402

[19] Koch S W, Hoyer W, Kira M and Filinov V S 2003 Exciton ionization in semiconductors *Phys. Status Solidi* b **238** 404–10

[20] Amo A, Martín M D, Viña L, Toropov A I and Zhuravlev K S 2006 Interplay of exciton and electron–hole plasma recombination on the photoluminescence dynamics in bulk GaAs *Phys. Rev.* B **73** 035205

[21] Deng H, Weihs G, Snoke D, Bloch J and Yamamoto Y 2003 Polariton lasing versus photon lasing in a semiconductor microcavity *Proc. Natl Acad. Sci. USA* **100** 15318–23

[22] Nelsen B, Balili R, Snoke D W, Pfeiffer L and West K 2009 Lasing and polariton condensation: two distinct transitions in GaAs microcavities with stress traps *J. Appl. Phys.* **105** 122414

[23] Balili R, Nelsen B, Snoke D W, Pfeiffer L and West K 2009 Role of the stress trap in the polariton quasiequilibrium condensation in GaAs microcavities *Phys. Rev.* B **79** 075319

[24] Tsotsis P, Eldridge P S, Gao T, Tsintzos S I, Hatzopoulos Z and Savvidis P G 2012 Lasing threshold doubling at the crossover from strong to weak coupling regime in GaAs microcavity *New J. Phys.* **14** 023060

[25] Tempel J-S *et al* Characterization of two-threshold behavior of the emission from a GaAs microcavity *Phys. Rev.* B **85** 075318

[26] Maragkou M, Grundy A J D, Ostatnický T and Lagoudakis P G 2010 Longitudinal optical phonon assisted polariton laser *Appl. Phys. Lett.* **97** 111110

[27] del Valle E, Sanvitto D, Amo A, Laussy F P, André R, Tejedor C and Viña L 2009 Dynamics of the formation and decay of coherence in a polariton condensate *Phys. Rev. Lett.* **103** 096404

[28] Deng H, Press D, Götzinger S, Solomon G S, Hey R, Ploog K H and Yamamoto Y 2006 Quantum degenerate exciton-polaritons in thermal equilibrium *Phys. Rev. Lett.* **97** 146402

[29] Kumar R, Vengurlekar A S, Prabhu S S, Shah J and Pfeiffer L N 1996 Picosecond time evolution of free electron–hole pairs into excitons in GaAs quantum wells *Phys. Rev.* B **54** 4891–7

IOP Institute of Physics Φ DEUTSCHE PHYSIKALISCHE GESELLSCHAFT

[30] Lin W Z, Fujimoto L G, Ippen E P and Logan R A 1987 Femtosecond carrier dynamics in GaAs *Appl. Phys. Lett.* **50** 124

[31] Zel'Dovich Ya B and Levich E V 1969 Bose condensation and shock waves in photon spectra *Sov. Phys.—JETP* **28** 1287–90

[32] Guillet T *et al* 2011 Laser emission with excitonic gain in a ZnO planar microcavity *Appl. Phys. Lett.* **98** 211105

[33] Lagoudakis P G, Martin M D, Baumberg J J, Malpuech G and Kavokin A 2004 Coexistence of low threshold lasing and strong coupling in microcavities *J. Appl. Phys.* **95** 2487–9

[34] Zou Z, Huffaker D L and Deppe D G 2000 Ultralow-threshold cryogenic vertical-cavity surface-emitting laser *IEEE Photon. Technol. Lett.* **12** 1–3

[35] Bernard M G A and Duraffourg G 1961 Laser conditions in semiconductors *Phys. Status Solidi* b **1** 699–703